19th Brazilian Congress of Thermal Sciences and Engineering
November 06th-10th, 2022, Bento Gonçalves - RS - Brazil

ENC-2022-0420
DETAILED ANALYSIS OF THE DIAMETER INFLUENCE ON AIR - WATER SLUG FLOW CHARACTERISTICS IN UPWARD VERTICAL FLOW

Paul Adrian Delgado Maldonado
Carolina Cimarelli Rodrigues
Eduardo Nunes dos Santos
Moises Alves Marcelino Neto
Marco José da Silva
Rigoberto E. M. Morales
Multiphase Flow Research Center – NUEM Federal Technological University of Parana – Av. Deputado Heitor Alencar Furtado, 5000, Curitiba, PR, Brazil
paul@alunos.utfpr.edu.br
carolcimarelli@gmail.com
e.n.santos@ieee.org
mneto@utfpr.edu.br
mdasilva@utfpr.edu.br
rmorales@utfpr.edu.br

Abstract. *Multiphase slug flow is found in pipes and process equipment in the oil & gas industry. Air-water slug flow is usually defined as the alternate passage of two structures: a liquid slug and a Taylor bubble, which is an elongated, bullet-shaped bubble. This type of flow occurs intermittently and the passage of all bubbles and liquid slugs have different lengths and velocities. The gas expansion in vertical multiphase flow is highly relevant, as it affects all the characteristic parameters. Therefore, the knowledge of the flow evolution and not only of its average behavior is essential to the design of separator equipment as well as pipelines. In this sense, this work aims to evaluate the influence of the internal diameter on the evolution of the characteristic parameters of slug flow such as the Taylor bubble velocity, the length of the elongated bubble and the liquid slug, the void fraction in bubble and slug regions, and the slug frequency. The experimental study was done in the Multilab experimental loop of the Multiphase Flow Center at UTFPR/NUEM with three different internal diameters (26, 40.8 and 50 mm). The entry section has a 10 m horizontal tube for flow development connected to a 90°-curve that directs the flow to the vertical test section with approximately 14 m of height. Fifty different combinations of air-water superficial velocities were used, of which twenty were for ID = 26 mm, twelve for ID = 40.8mm and eighteen for ID = 50 mm. To evaluate the flow, five measuring stations were used: four two-wire resistive sensors and one wire-mesh capacitive sensor. The pressure was measured at the five measuring stations with differential/gauge pressure transmitters and an atmospheric pressure transmitter was used. High image acquisition camera were used to analyze the flow qualitatively in three different heights in order to acquire the largest number of relevant images from the slug flow. The results obtained provided valuable information for the development of models/simulators and engineering correlations that allow an accurate prediction of the evolution of slug flow in vertical pipes.*

Keywords: *vertical slug flow, evolution of air-water slug flow, diameter influence in slug flow*

1. INTRODUCTION

Vertical slug flow occurs in a wide range of engineering applications, such as exploitation of oil and natural gas, nuclear and chemical reactors and heat exchangers. More details about practical applications can be found on the review published by Morgado et al., (2016) about vertical slug flow. In Oil & Gas industry, it occurs during the production and transportation of oil-gas mixtures. In these scenarios, there is a significant pressure gradient along the liquid column; hence, the prediction of pressure drop and gas–liquid spatial distribution in the pipeline is pivotal in the design of separators or even in predicting the flow behavior along the pipeline. Those variables require proper knowledge of the characteristic hydrodynamic parameters.

Slug flows are characterized by the intermittent passage of two structures: an elongated bubble (known as the Taylor bubble) whose length exceeds a pipe diameter, followed by the passage of a liquid body known as the liquid slug (Davies e Taylor, 1950). Those two structures compose a slug unit-cell and, for modelling purpose, the slug flow can be simplified as a series of identical representative unit-cells travelling with a velocity equal to the translational bubble velocity U_{TB}.

Over the years, a number of authors have dealt with such unit-cell models, e.g., Dukler & Hubbard (1975) and Nicholson et al. (1978) for horizontal cases; Fernandes et al. (1983), Sylvester (1987), and Orell & Rembrand (1986) for vertical configurations; Bonnecaze et al. (1971) for inclined situations, and Taitel & Barnea (1990) for all inclinations.

The unit-cell modelling is based on two constitutive balance equations, the mass and the momentum equations. Several additional closure laws are needed to close the system and to ensure a physical solution to the problem. Steady models give an estimate of averaged flow values, and those values can be used as initial conditions for two-fluid transient models. However, knowledge of those averaged values alone may be inadequate due to the lack of information about the longitudinal distribution of the flow, which is sometimes essential. Slug catchers, which should remove slugs from pipelines, are for example designed based on the maximum slug length value and not the average value.

As the slug flow has the characteristic of a stochastic phenomenon, it varies randomly both in time and space. Complete description of slug flow hydrodynamics includes the mean flow parameters, such as characteristic velocities of propagation of liquid–gas interfaces, the characteristic lengths and shapes of elongated bubbles and liquid slugs, the distribution of the shear stresses along the slug unit and the spatial distribution of the void fraction in the liquid slug (Shemer, 2003).

The evolution of slug flow along a pipeline strongly depends on the relative velocities between the elongated bubbles. At short separation distances, trailing elongated bubbles accelerate and eventually merge with the leading ones (Moissis and Griffith, 1962; Pinto et al., 1998; Aladjem Talvy et al., 2000). During the merging process, both the liquid slug and the elongated bubble lengths increase. This coalescence process may occur until the liquid velocity profiles at the back of the liquid slug are fully developed and all elongated bubbles propagate at the same translational velocity.

Most experimental research concerning length distributions have been focused on determining the mean and maximum liquid slug lengths. Mean liquid slug lengths were found to be relatively independent of flow rates. For vertical slug flow, the mean liquid slug lengths experimentally measured and normalized by the pipe diameter lie in the range from 10 to 20 with standard deviations between 30% and 50% (Griffith and Wallis, 1961; Barnea and Shemer, 1989; van Hout et al., 1992, 2001; Nydal et al., 1992; Costigan and Whalley, 1997). For the horizontal case, reported mean liquid slug lengths vary between 10 and 100D (Nydal et al., 1992; Andreussi et al., 1993). Taitel e Barnea (1993) showed that for fully developed slug flow the mean slug length is about 1.5 times the minimum stable slug length and the maximum length is about 3 times the minimum stable slug length.

As presented above, many papers about vertical liquid-gas slug flow focus on mean values to characterize the structures in the flow. Information about the distribution of these parameters and evolution of the flow along the pipe regarding the influence of the pipe diameter is scarce, although essential for developing reliable models for the prediction of vertical slug flow. The aim of the present investigation is to evaluate the diameter influence on the evolution of the hydrodynamic and statistical parameters of slug flow. Therefore, experiments with three different diameters were studied in order to analyze the liquid slug and Taylor bubble length distribution, as well as the Taylor bubble translational velocity and the unit-cell frequency in five different measuring stations.

2. EXPERIMENTAL METHODOLOGY

The experimental study was developed in the Multilab experimental loop of the Multiphase Flow Center at UTFPR/NUEM with three internal diameters (26, 40.8 and 50 mm). The inlet section is a horizontal tube with a length (LE) of 10.7 m for flow development, which is connected to a 90°-curve that directs the flow to the vertical test section with 14.3 m of height. The experimental facility was built with a horizontal inlet section, instead of only vertical flow, because it helps on the development of the vertical slug flow. With the horizontal section, the Taylor bubbles that arrive on the 90°-curve already have a considerable size, causing the coalescence process at the beginning of the vertical section to accelerate.

The instruments used to monitor the experiment are four two-wire resistive sensors (S1, S2, S4, S5) and one wire-mesh capacitive sensor (S3) shown in Fig. (1). The sensor methodologies can be found in Dos Santos et al. (2018) and Da Silva et al. (2007), respectively. The acquisition rate of the resistive sensors was 1,000 Hz, and 2,000 Hz for wire-mesh sensor. The sensors are in the vertical test section and the distances between them are indicated in Tab. (1), where D1, D2, and D3 refer to the internal diameters of 26, 40.8 and 50 millimeters, respectively. The distances between the sensors in Fig. (1) are depicted in Tab. (1), where LS1 refers to the distance between the 90º-curve and S1 in the test section; LS2 to LS5 are the distances between the sensors S1-S2, S2-S3, S3-S4, S4-S5, respectively, and LS6 is the distance between S5 and the flow output curve where the flow is directed to the flow attenuator and phase separator.

The two sections, horizontal and vertical, are made of transparent acrylic pipe to facilitate the observation of the development of the flow. The inlet section is fed by two lines, one for liquid and the other for compressed air that are combined in the mixer.

Pressure drop was monitored along the pipe by means of SCADA (Supervisory Control and Data Acquisition). The atmospheric pressure and temperature was monitored during the experiments. The reference value of the gas superficial velocity was adjusted for each test at the reference station (Sref), shown in Fig.(1).

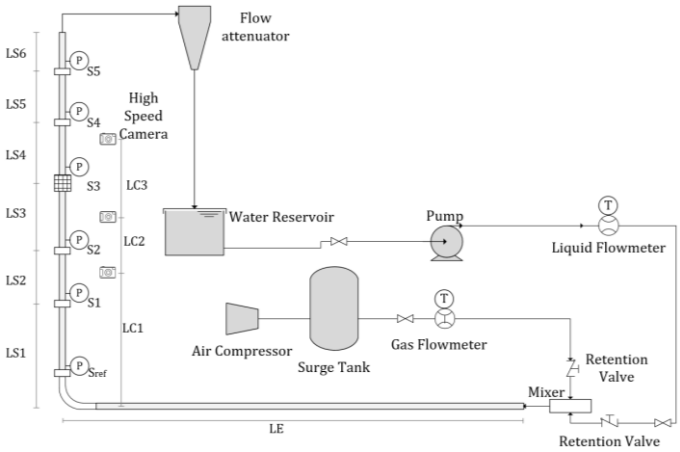

Figure 1. Schematic diagram of the Multiphase loop facility.

Table 1. Distance between each sensor for each internal diameter used.

	D1	D2	D3		D1	D2	D3
LS1 [m]	3.909	4.039	4.040	LS6 [m]	3.010	2.615	2.615
LS2 [m]	1.800	1.888	1.887	LC1 [m]	0.544	3.739	3.740
LS3 [m]	2.123	2.302	2.302	LC2 [m]	7.532	7.929	7.929
LS4 [m]	1.799	1.882	1.882	LC3 [m]	10.647	11.042	11.042
LS5 [m]	1.616	1.531	1.531	LE [m]	10.637	10.637	10.637

A high-speed camera was used to analyze the flow qualitatively at three different elevations to acquire the largest number of relevant images from the slug flow, see Fig. (2).

Table 2. Combinations of air-water superficial velocities

	D1		D2		D3	
	J_G [m/s]	J_L [m/s]	J_G [m/s]	J_L [m/s]	J_G [m/s]	J_L [m/s]
P01	0.3	0.3	0.5	0.5	0.4	0.4
P02	0.2	0.4	0.6	0.4	0.3	0.5
P03	0.4	0.2	0.4	0.6	0.5	0.3
P04	0.4	0.4	0.75	0.75	0.5	0.5
P05	0.3	0.5	1.0	0.5	0.6	0.4
P06	0.5	0.3	0.5	1.0	0.4	0.6
P07	0.5	0.5	1.0	1.0	0.75	0.75
P08	0.3	0.7	1.3	0.7	1.0	0.5
P09	0.7	0.3	0.7	1.3	0.5	1.0
P10	0.6	0.6	1.25	1.25	1.0	1.0
P11	0.8	0.4	1.7	0.8	1.3	0.7
P12	0.4	0.8	0.8	1.7	0.7	1.3
P13	0.75	0.75			1.25	1.25
P14	1.0	0.5			1.7	0.8
P15	0.5	1.0			0.8	1.7
P16	1.0	1.0			1.5	1.5
P17	0.5	1.5			1.0	2.0
P18	1.5	0.5			2.0	1.0
P19	1.3	0.7				
P20	0.7	1.3				

In this study, fifty different combinations of air-water superficial velocities for gas and liquid (J_G and J_L) were used, of which twenty were for ID = 26 mm, twelve for ID = 40.8 mm, and eighteen for ID = 50 mm. The combinations of air-water superficial velocities are presented in Tab. (2). Each experimental condition was tested three times to verify the repeatability.

The testing grid was established by using the Taitel's flow map (1980) as reference, to find the flow rates required for slug flow in vertical pipe.

3. RESULTS AND DISCUSSION

The pipe diameter influences the slug flow hydrodynamics in several aspects and those will be discussed following. Figure 2 shows the behavior of the Taylor bubble for the same gas/liquid superficial velocity pair, J_G = 0.7 m/s and J_L = 1.0 m/s, for three different diameters. The high-speed images depict in details the aeration in the liquid slug and how it increases with the diameter. The higher the aeration, the harder to identify the bubble nose location. This visual obstruction also happens when the mixture velocity (J) is high, making it challenging to identify the beginning and the end of the elongated bubbles because of the high concentration of the dispersed bubbles.

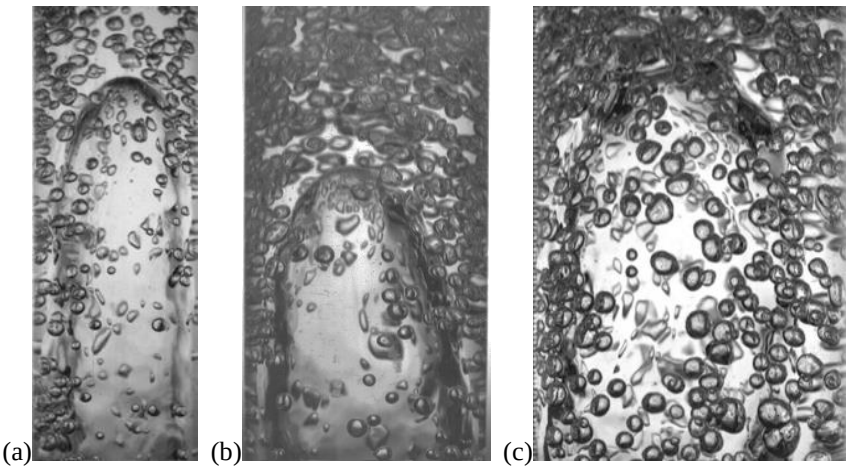

Figure 2. Images taken from the high-image acquisition camera, detail of the passage of a Taylor elongated bubble nose for (a) 26, (b) 40.8 and (c) 50 mm ID

Another behavior visualized with the images obtained, is the instability of the shape of the bubble nose and its relationship with the mixture velocity. As J increases, the shape of the bubble nose become more pointed and irregular. Similarly, the end of Taylor's bubble and wake region exhibits increasingly disordered behaviors as J increases. This behavior of instability of the structures is directly related to the increase in the flow inertia and turbulence.

The slug flow characteristic parameters (bubble velocity, bubble and slug lengths and the unit cell frequency) were obtained from a statistical analysis of the experiments. Herein, they are presented as PDFs (Probability Density Function) of the different variables. With this kind of representation, it is possible to visualize the distribution and behavior of the variable globally, and not only as an average value, therefore ensuring that the behavior of the variable is correctly represented. From the results of the five stations, correlations for mean values were also obtained for each of the characteristic parameters of the vertical slug flow.

3.1 Bubble nose velocity (V_{TB})

The velocity of the Taylor bubble nose is one of the essential parameters in slug flow modeling, as it is a closure relationship. The result presented for this parameter, Fig. (3), refers to P15 (J_G=0.5 m/s and J_L=1.0 m/s) and D1 (26 mm). Velocity values tend to increase along the pipe, and PDF behavior becomes a normal distribution, in agreement with literature observations publish by Van Hout (2002) and Shemer (2003) among others.

In general, the bubble velocity distributions showed higher peaks at the first stations, indicating that the velocity values in the beginning of the vertical test section variated less than in the stations near the flow outlet. For example, in station S1 the values vary between 1.9 and 2.1 m/s. On the other hand, the results for S5 vary between 2.1 and 2.5 m/s approximately, showing a higher variation of the bubble nose velocity and with it a greater difficulty for the flow to stabilize. This higher variation can be a result of the bubble expansion that causes a displacement of the liquid ahead of the bubble letting to an additional contribution to the liquid velocity of its nose ahead of the bubble. Therefore this mechanism causes an acceleration of the bubble nose velocity which could let to an increase of velocity variation.

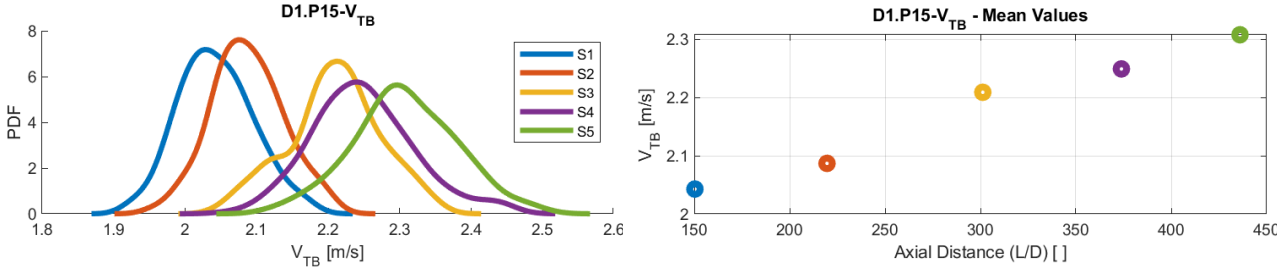

(a) (b)

Figure 3. (a) Bubble nose velocity distribution for P15 in D1 and (b) mean values.

The correlation for the bubble nose velocity, show in Eq. (1), was obtained from all the average results for the entire grid test presented in Tab. (2). Equation (1) is defined in function of the Froude number ($Fr_J = J/\sqrt{gd}$), the internal diameter (D) and the force of gravity (g) with a coefficient of determination (R^2) of 0.99.

$$V_{TB} = \sqrt{gD}\left(1.249Fr_J + 0.1877\right) \tag{1}$$

Equation (1) is presented following the way Bendicksen (1984) presents the model of the terminal velocity for the elongated bubble in slug flow. In this way it is possible to identify that for the experiments performed in this work the value obtained for the distribution constant (C_0) is 1.249, and for the drift velocity coefficient (C_∞) the obtained value was 0.1877. This values are very close to those presented in the literature that are 1.2 and 0.35, respectively.

Figure 4 shows a comparison between experimental results and the correlation given by Eq. (1) with a relative error of 5%. The mean relative error between the experimental results and those obtained by Eq. (1) were 3.1%, with max errors of approximately 25%.

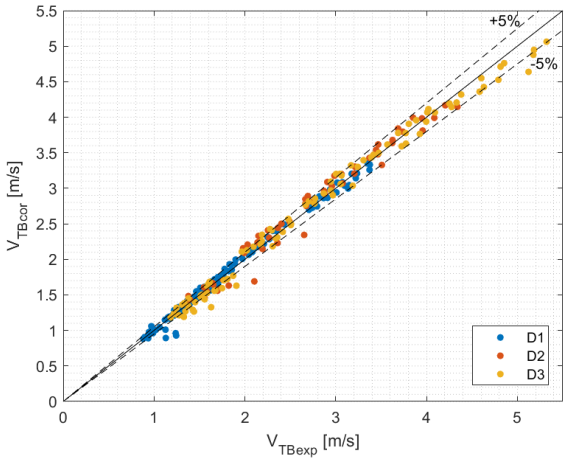

Figure 4. Predicted performance of bubble nose velocity correlation with the experimental data.

Figure 4 shows some results that could be considered as outliers. These results were identified in the experimental points P03 of D1 and P05 of D3. The characteristic of these experimental points is the high amount of gas for low mixture velocities. These superficial velocity combinations are within the envelope shown by the Taitel's flow map (1980) for vertical multiphase flow, but due to the configuration of the experimental facility, these combinations of superficial gas (J_G) and liquid (J_L) velocities are very close to the transition between slug and stratified flow on the flow map for horizontal multiphase flow. This causes a liquid accumulation in the region of the curve section from the horizontal to vertical, forming a severe slug that expels the entire liquid. This behavior was already reported by Taitel (1986) in slightly inclined tube configurations directing the stratified flow to risers in vertical position.

3.2 Bubble length (L_B)

The lengths of the elongated bubbles increased as the flow advanced in the vertical tube, as shown in Fig. (5). The result presented for this parameter refers to P08 (J_G=1.3 m/s and J_L=0.7 m/s) and D2 (40.8 mm). This behavior was expected since the elongated Taylor bubble has constant growth due to the gas expansion as the pressure drops (Campos et al., 2006).

From Fig. (5.a) it is possible to identify an increasing bimodal behavior: starting at station S2 and evolving to a plateau in S3, S4 and S5 stations, flattening the curve, displaying a high occurrence of small and large elongated bubbles as well.

This bimodal behavior, only noticed with the PDF distribution charts, can be an indication of a Taylor bubble's coalescence, causing smaller bubbles to accelerate and coalesce with the larger bubble in front.

The results obtained for lower mixture velocities (J<1 m/s) presented bubble length along the test line that was not continually increasing. Despite the expansion of the gas, the length on the next sensor was not always larger than the one behind. One possible explanation for this behavior is the accumulating liquid on station closer to the outlet, which causes the liquid inertia to decrease and therefore the drainage mechanism to increase around the Taylor bubble, sometimes causing bubbles to break and new liquid slugs to form.

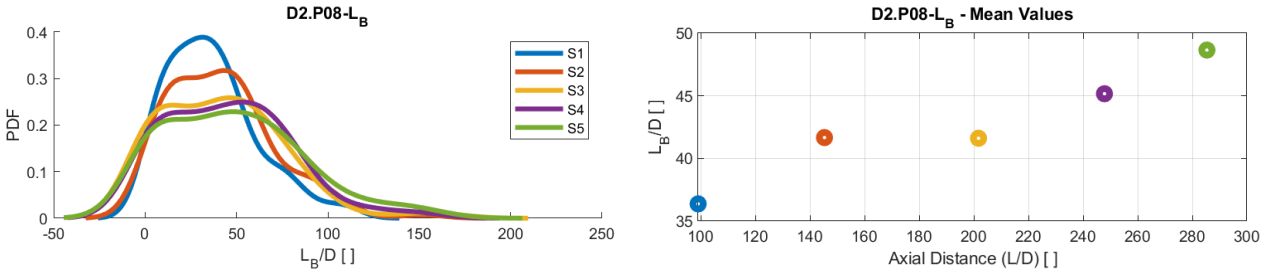

(a) (b)

Figure 5. (a) Bubble length distribution for P08 in D2 and (b) mean values.

The correlation equation for the bubble length shown in Eq. (2) was developed from all the average results obtained for the entire grid test as presented in Tab. (2). Equation (2) is defined as function of the superficial velocities of air and the mixture velocity ($J = J_L + J_G$), and the diameter (D) with a coefficient of determination (R^2) of 0.89.

$$L_B = D\left(0.6785 \exp\left(5.822 \frac{J_G}{J}\right)\right) \tag{2}$$

The behavior of the exponential curve relating the amount of gas inside the tube has a direct relationship with the length of the bubble. Therefore, as the superficial velocity of the gas increases in relation to the liquid, the Taylor bubbles length tends to enlarge rapidly. The correlation comparison between experimental results and Eq. (2) is shown in Fig. (6) with a relative error of 20%.

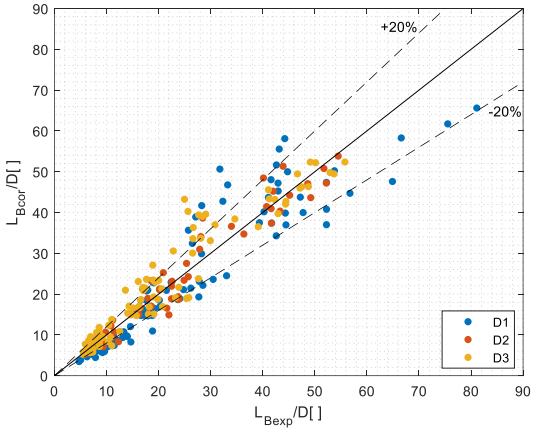

Figure 6. Predicted performance of the bubble length correlation with the experimental data.

The mean relative error between the experimental results and those obtained by Eq. (2) were 13.3%, with max errors of approximately 50%.

3.3 Unit cell Frequency (f)

The frequency is calculated as function of each valid unit cell and the time passage of this structure. The frequency distribution is shown in Fig. (7). It refers to P10 (J_G=1.0 m/s and J_L=1.0 m/s) in D3 (50 mm) and has a decay behavior of the harmonic mean values as the flow advances in the tube. This can be explained on the grounds of an increase in the size of the structures (L_B) which decreases the frequency of the unit cell at the stations closer to the flow outlet, and also the coalescence mechanism that exist in the beginning of the vertical slug flow, where the liquid slug length are note well established.

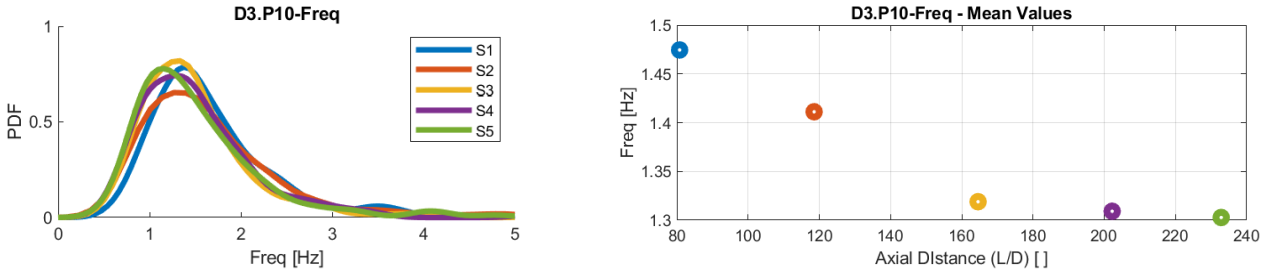

(a) (b)

Figure 7. (a) Unit cell frequency distribution for P10 in D3 and (b) mean values.

From the frequency distribution, it was possible to observe that all the stations have similar variations and although the mean value decreases as the axial distance increases, the frequency values that occur more frequently remained within a narrow range.

Due to the increase in the unit cell size, as a result of the gas expansion, the slug flow frequency presents a tendency to decrease. In the first stages, where the flow is less stablished, the passage of short liquid slugs (up to 8D) is predominant, which was also reported by Costigan and Whaley (1997). This shows that the coalescence of elongated bubbles occurs mostly and has greater influence in the first stations, where it was either an entrance region or a slug flow development region, than in the stations closer to the outlet of the flow.

The correlation equation for the unit cell frequency shown in Eq. (3) was developed from all the average results obtained for the entire grid test presented in Tab. (2) and is defined in terms of the superficial velocities of gas and liquid, and the internal diameter (D) with a coefficient of determination (R^2) of 0.95. The comparison with experimental results is shown in Fig. (8) with a relative error of 30%.

$$f = 0.005177 \frac{J_G}{D} \exp\left(5.301 \frac{J_L}{J}\right) \tag{3}$$

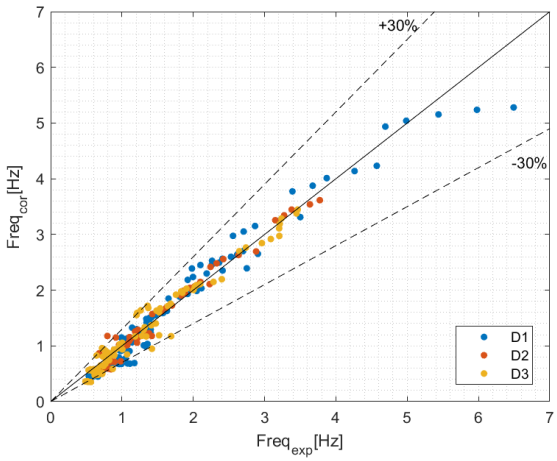

Figure 8. Predicted performance of the Unit cell Frequency correlation with the experimental data.

The mean relative error between the experimental results and those obtained by Eq. (3) were 7.2%, with max errors of approximately 30%.

3.4 Slug Length (L_S)

The length of the liquid slugs increases as the flow advance in the vertical tube, as shown in Fig. (9). The result presented for this characteristic parameter is from the experimental point P12 (J_G=0.7 m/s, J_L=1.3 m/s) for D3 (50 mm). In the same way as the length behavior of Taylor's bubbles, the liquid slug length increases and for the overall distribution the slug length varies mostly between 10D and 40D as reported in literature (Fernandes, 1981; Barnea and Shemer, 2003; Costigan and Whalley, 1997).

The distribution of the void fraction along the liquid slug shows that the agglomeration of dispersed bubbles are located just downstream the wake region. This is due to the drag of small bubbles that are pulled from the wake region due to the high velocity of the liquid in the film region around Taylor's bubble. These dispersed bubbles are very small as their Eötvös number, showing a high surface tension force, which makes the coalescence of these bubbles hindered, even with a high collision occurrence between them.

The increase in the length of the elongated bubbles is also caused because of the development and stabilization of the slug flow, which is directly related to the length of the liquid slug. The liquid slug must be sufficiently long which the liquid velocity profile does not interfere with the velocity profile of the elongated bubbles before and after the liquid slug. This length is to be approximately 16D (Taitel, 1980).

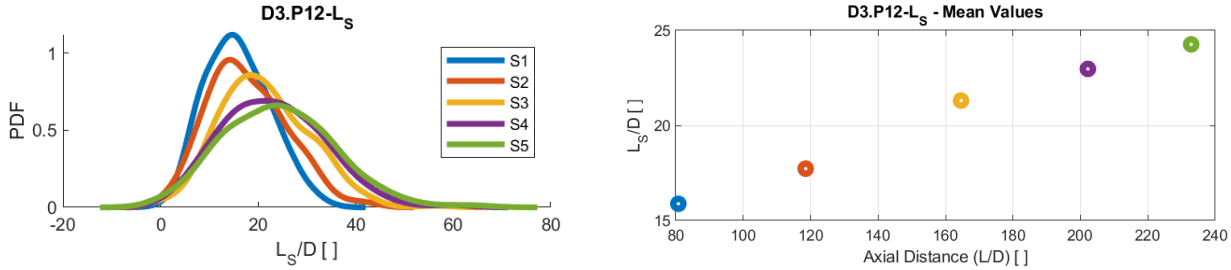

(a) (b)

Figure 9. (a) Bubble length distribution for P12 in D3 and (b) mean values.

The equation found for the slug length parameter was better adjusted using the intermittency factor, defined by the ratio of the elongated bubble length to the sum of the elongated bubble and liquid slug lengths ($\beta = L_B/(L_B + L_S)$). The intermittence factor correlation found with the experimental results with a regression technique is presented in Eq. (4), and has a coefficient of determination (R^2) of 0.81.

$$\beta = 0.1304 \exp\left(2.124 \frac{J_G}{J}\right) \tag{4}$$

The correlation found for the intermittency factor was obtained as a function of the mixture velocity (J) and the air superficial velocity (J_G). Equation (4) was plotted and compared with the mean results, obtained from the intermittency coefficient for all experimental points, shown in Fig. (10).

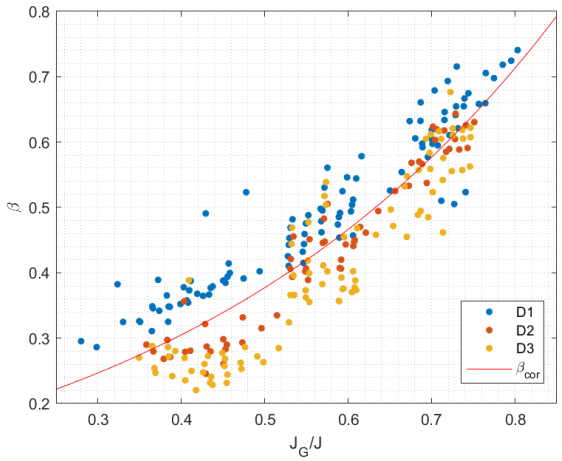

Figure 10. Predicted correlation found for intermittency factor (β) and the experimental results obtained for β.

The equation for the slug length parameter is defined in Eq. (5) and Eq. (6). The variables used in Eq. (6) were previously defined in Eq. (1) for the bubble velocity (V_{TB}), Eq. (3) for unit cell frequency (f) and Eq. (4) for the intermittency factor (β).

$$\frac{L_S}{D} = \frac{1}{D}\left[\frac{V_{TB}}{f} - L_B\right] \tag{5}$$

$$L_S = \frac{V_{TB}}{f}(1 - \beta) \tag{6}$$

The mean relative error between the experimental results and those obtained by Eq. (6) were 13.6%, with max errors of approximately 45%. Equation (6) is defined within function of the bubble nose velocity (Eq. (1)), unit cell frequency (Eq. (3)) and the intermittency factor (Eq. (4)), all presented in this paper.

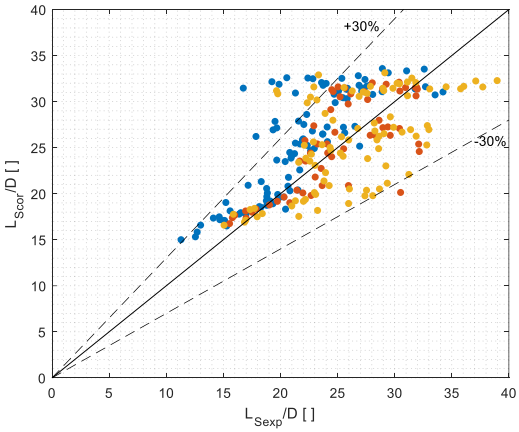

Figure 11. Predicted performance of the Slug Length correlation with the experimental data.

Most divergences between the experimental results and the results obtained by Eq. (6) refer to large liquid slugs. In large slugs, the passage of bubbles similar to Taylor's, but with length less than 2D, were identified. These bubbles were considered as spherical cap bubbles, i.e. not Taylor bubbles, causing the piston reading to be recorded higher than the average of the experimental point.

The length of the liquid slugs are directly proportional to the magnitude of the nose velocity of the Taylor bubble, but this comes along with the difficulty of identifying each of the unit cell structures, due to piston aeration. Therefore, the results founded by Eq (6) tend to higher values of piston length, on the other hand, the results obtained by the experimental means present lower results.

4. CONCLUSIONS

The results obtained by the experiments herein presented showed great worth when it comes to understanding the phenomena involved with the evolution of the vertical slug flow.

From the experiments, it is possible to claim that the behavior of the characteristic parameters presents values that may be far from the values obtained by the mean, showing the importance of the deviation of the variables and its distribution for a better understanding of the phenomenon.

The proposed correlations can be used for the different diameters within mean relative errors of 3.1% for bubble nose velocity in Eq (1), 13.3% for Taylor bubble length in Eq. (2), 7.2% for unit cell frequency in Eq. (3), and 13.6% for slug length in Eq. (6).

A new correlation is presented for the intermittency factor (β) correlating the behavior of the size of the unit cell structures with a coefficient of determination (R^2) of 0.8073.

The identification of unit cell structures is still a difficulty task, either by the type of data processing or by the limitation of the sensor used. However, with the probability distribution (PDF) of each of the parameters obtained it is possible to identify values that are far out of the mean, considered as outliers; or even values considered as false identification.

5. REFERENCES

Andreussi, P., Bendiksen, K. H., & Nydal, O. J. (1993). Void distribution in slug flow. International Journal of Multiphase Flow, 19(5), 817-828.

Barnea, D., & Shemer, L. (1989). Void fraction measurements in vertical slug flow: applications to slug characteristics and transition. International Journal of Multiphase Flow, 15(4), 495-504.

Barnea, D., and Y. Taitel. "A model for slug length distribution in gas-liquid slug flow." International Journal of Multiphase Flow 19.5 (1993): 829-838.

Bendiksen, K. H. (1984). An experimental investigation of the motion of long bubbles in inclined tubes. International journal of multiphase flow, 10(4), 467-483.

Bonnecaze B., W Eriskine Jr., E.J Greskovich. Holdup and pressure drop for two-phase slug flow in inclined pipelines. AIChE J., 17 (1971), pp. 1109-1113

Costigan, G., & Whalley, P. B. (1997). Slug flow regime identification from dynamic void fraction measurements in vertical air-water flows. International Journal of Multiphase Flow, 23(2), 263-282.

Davies, R. M., Taylor G. I.. "The mechanics of large bubbles rising through extended liquids and through liquids in tubes." Proceedings of the Royal Society of London. Series A. Mathematical and Physical Sciences 200.1062 (1950): 375-390.

Da Silva, M. J., E. Schleicher, and U. Hampel. "Capacitance wire-mesh sensor for fast measurement of phase fraction distributions." Measurement Science and Technology 18.7 (2007): 2245.

Dos Santos, E. N., et al. "Sensing platform for two-phase flow studies." IEEE Access 7 (2018): 5374-5382.

Dukler, A. E., & Hubbard, M. G. (1975). A model for gas-liquid slug flow in horizontal and near horizontal tubes. Industrial & Engineering Chemistry Fundamentals, 14(4), 337-347.

Fernandes, R. C., Raphael Semiat, and Abraham E. Dukler. "Hydrodynamic model for gas-liquid slug flow in vertical tubes." AIChE Journal 29.6 (1983): 981-989.

Gregory, G. A., Nicholson, M. K., & Aziz, K. (1978). Correlation of the liquid volume fraction in the slug for horizontal gas-liquid slug flow. International Journal of Multiphase Flow, 4(1), 33-39.

Griffith, P., & Wallis, G. B. (1961). Two-phase slug flow. Journal of Heat Transfer, 83(3).

Moissis, R., & Griffith, P. (1962). Entrance effects in a two-phase slug flow.

Morgado, A. O., et al. "Review on vertical gas–liquid slug flow." International Journal of Multiphase Flow 85 (2016): 348-368.

Nydal, O. J., Pintus, S., & Andreussi, P. (1992). Statistical characterization of slug flow in horizontal pipes. International journal of multiphase flow, 18(3), 439-453.

Orell, A., & Rembrand, R. (1986). A model for gas-liquid slug flow in a vertical tube. Industrial & engineering chemistry fundamentals, 25(2), 196-206.

Pinto, A. M. F. R., Pinheiro, M. C., & Campos, J. B. L. M. (1998). Coalescence of two gas slugs rising in a co-current flowing liquid in vertical tubes. Chemical engineering science, 53(16), 2973-2983.

Shemer, Lev. "Hydrodynamic and statistical parameters of slug flow." International journal of heat and fluid flow 24.3 (2003): 334-344.

Sousa, R. G., A. M. F. R. Pinto, and J. B. L. M. Campos. "Effect of gas expansion on the velocity of a Taylor bubble: PIV measurements." International journal of multiphase flow 32.10-11 (2006): 1182-1190.

Sylvester, N. D. "A mechanistic model for two-phase vertical slug flow in pipes." (1987): 206-213.

Taitel, Y., Barnea D., and Dukler A. E.. "Modelling flow pattern transitions for steady upward gas-liquid flow in vertical tubes." AIChE Journal 26.3 (1980): 345-354.

Taitel, Y. "Stability of severe slugging." International journal of multiphase flow 12.2 (1986): 203-217.

Taitel, Y., & Barnea, D. (1990). Two-phase slug flow. In Advances in heat transfer (Vol. 20, pp. 83-132). Elsevier.

Talvy, C. A., Shemer, L., & Barnea, D. (2000). On the interaction between two consecutive elongated bubbles in a vertical pipe. International Journal of Multiphase Flow, 26(12), 1905-1923.

Van Hout, R., D. Barnea, and L. Shemer. "Translational velocities of elongated bubbles in continuous slug flow." International Journal of Multiphase Flow 28.8 (2002): 1333-1350.

Van Hout, R., L. Shemer, and D1 Barnea. "Evolution of hydrodynamic and statistical parameters of gas–liquid slug flow along inclined pipes." Chemical Engineering Science 58.1 (2003): 115-133

6. RESPONSIBILITY NOTICE

The authors are the only responsible for the contents and opinions expressed in this article.